

Two-Dimensional Structured-Compressed-Sensing-Based NBI Cancellation Exploiting Spatial and Temporal Correlations in MIMO Systems

Sicong Liu, *Student Member, IEEE*, Fang Yang, *Senior Member, IEEE*, Wenbo Ding, *Student Member, IEEE*, Xianbin Wang, *Senior Member, IEEE*, and Jian Song, *Fellow, IEEE*

Abstract—Narrowband interference (NBI) caused by narrowband licensed or unlicensed services is a major concern that constrains the performance of multiple-input multiple-output (MIMO) systems. In this paper, the new and powerful signal processing theory of structured compressed sensing (SCS) is introduced to solve this problem. Exploiting the 2-D spatial and temporal correlations of NBI in MIMO systems, a novel NBI recovery method, i.e., the spatial multiple differential measuring method, is proposed in the framework of 2-D SCS. At each receive antenna, a differential measurement vector is acquired from the repeated training sequences in the IEEE 802.11 series preamble. Then, multiple measurement vectors from all receive antennas are utilized to recover and cancel NBI using the proposed SCS greedy algorithm of structured sparsity adaptive matching pursuit. Simulation results indicate that the proposed scheme outperforms the conventional schemes over the wireless MIMO channel.

Index Terms—Multiple-input multiple-output (MIMO), narrowband interference (NBI), spatial and temporal correlations, two-dimensional (2-D) structured compressed sensing (SCS).

Manuscript received August 31, 2015; revised November 26, 2015; accepted January 4, 2016. Date of publication January 6, 2016; date of current version November 10, 2016. This work was supported in part by the National Natural Science Foundation of China under Grant 61401248 and Grant 61471219, by the New Generation Broadband Wireless Mobile Communication Network of the National Science and Technology Major Projects under Grant 2015ZX03002008, by the Tsinghua University Initiative Scientific Research Program under Grant 2014Z06098, and by the Science and Technology Project of State Grid Corporation of China under Grant SGHAZZ00FCJS1500238. The review of this paper was coordinated by Prof. W. A. Hamouda.

S. Liu and W. Ding are with the Research Institute of Information Technology and the Department of Electronic Engineering, Tsinghua University, Tsinghua National Laboratory for Information Science and Technology (TNList), Beijing 100084, China (e-mail: liu-sc12@mails.tsinghua.edu.cn; dwb11@mails.tsinghua.edu.cn).

F. Yang and J. Song are with the Research Institute of Information Technology and the Department of Electronic Engineering, Tsinghua University, Tsinghua National Laboratory for Information Science and Technology (TNList), Beijing 100084, China, with the National Engineering Laboratory for DTV (Beijing), Beijing 100191, China, and also with the Shenzhen City Key Laboratory of Digital TV System (Guangdong Province Key Laboratory of Digital TV System), Shenzhen 518057, China (e-mail: fangyang@tsinghua.edu.cn; jsong@tsinghua.edu.cn).

X. Wang is with the Department of Electrical and Computer Engineering, University of Western Ontario, London, ON N6A 5B9, Canada (e-mail: xianbin.wang@uwo.ca).

Color versions of one or more of the figures in this paper are available online at <http://ieeexplore.ieee.org>.

Digital Object Identifier 10.1109/TVT.2016.2515132

I. INTRODUCTION

THE multiple-input multiple-output (MIMO) technique is widely applied in various broadband communications systems, such as the wireless local area network (WLAN) specified in the IEEE 802.11 series standards [1] and the wireless access in vehicular environments specified in the IEEE 802.11p standard [2], to utilize spatial diversity and improve system capacity. To overcome severe channel conditions, orthogonal frequency-division multiplexing (OFDM) has been adopted in wireless MIMO systems [1], [2]. However, the OFDM-based MIMO systems, including WLAN and wireless access in vehicular environment systems, suffer from various noise levels such as the non-Gaussian narrowband interference (NBI). NBI is generated by licensed service or unlicensed (intended or unintended) signals in the same band. There can be multiple interferers in the same band, making the NBI a superposition of tone interferers. For instance, the WLAN system is prone to the licensed narrowband Bluetooth signal that shares the same band with the WLAN [3]. The wireless access in the vehicular environment system specified by the IEEE 802.11p standard also suffers from narrowband disruptions [4]. Narrowband radio emissions from some electric devices such as microwave ovens will generate NBI impacts on wireless systems [5]. The narrowband harmonics noise levels from personal computers generate NBI that has impacts on wireless OFDM systems [6]. The narrowband broadcast signal and amateur radio could introduce very harmful impacts to the subcarriers of digital subscriber line or power line communications [7], [8]. NBI causes a severe impact on the synchronization and demodulation performance at the receiver [9], [10]. Moreover, the NBI is mixed with the transmitted signal in both the time and frequency domains, making it very difficult to measure or mitigate [11]. According to thorough literature investigation, the state-of-the-art-related research on NBI mitigation for MIMO systems is still quite inadequate, nor is the temporal or spatial correlation of the NBI fully exploited for NBI mitigation. Hence, it is important to design an effective method of NBI mitigation for MIMO systems.

Some state-of-the-art NBI mitigation methods have been studied in [12]–[14]. For instance, a time–frequency interleaving scheme aimed at mitigating NBI is proposed to provide large time and frequency diversities [12]. The conventional

frequency threshold excision approach detects and then excludes the subcarriers with power larger than the threshold [13]. Through linear minimum-mean-square-error estimation, NBI signal is subtracted with the aid of the preserved virtual subcarriers [14], whereas the positions of virtual subcarriers have to be set around the NBI-contaminated subcarriers. Unfortunately, conventional methods passively mitigate the NBI, which means that they try to relieve the degradation caused by the NBI through excision or filtering that cannot exactly recover and cancel the true interference, leading to a reduction in OFDM system capacity.

The frequency-domain NBI signal is modeled as a long vector with as many entries as the OFDM subcarriers, and only a few of them are nonzero entries; hence, the frequency-domain NBI is a high-dimensional sparse vector. Since the length of the NBI vector is quite long, it is difficult to acquire sufficient sampling data for estimation using conventional methods. The powerful newly emerging technique in signal processing, i.e., compressed sensing (CS) [15], proffers a novel solution to NBI estimation since the NBI is naturally sparse in the frequency domain. However, how to acquire the CS measurement vector of the NBI is still a difficult problem since the NBI is mixed with transmitted data and/or training sequences in both time and frequency domains. The CS theory is first introduced to NBI mitigation in [16], where the measurement vector is acquired from the null space of the channel transfer matrix. As another branch of CS-based NBI recovery methods, a simple and effective method of temporal differential measuring (TDM) is presented to acquire the measurement vector for NBI recovery in our previous work [4], but the NBI is processed by the classical CS method at only one single receive antenna without exploiting the possible spatial correlation, which is not stable enough and might degrade in severe conditions of the NBI. Consequently, the current research on CS-based NBI recovery is still far from adequate.

To overcome the drawbacks of conventional NBI mitigation techniques and the classical CS-based method in our previous work [4], this paper focuses on the accurate and stable NBI recovery for MIMO systems for the first time by the development and application of the extension of the classical CS theory, i.e., the structured CS (SCS) theory [17]. The 2-D spatial and temporal correlations are also first exploited in this paper to facilitate the SCS-based method. The main novel contributions of this paper with respect to the state-of-the-art methods are as follows.

- The method of spatial multiple differential measuring (SMDM) is proposed to obtain the SCS measurement matrix of the NBI for MIMO systems, which has not been reported in the literature. It is noted that in MIMO systems, the superposition of different training sequence components at any receive antenna is of a strictly repeating structure independent of the multipath channel so that the NBI temporal correlation can be fully exploited to obtain the measurement data accurately through a simple differential operation.
- The 2-D temporal and spatial correlations of the NBI are utilized to constitute the SCS optimization model for the first time using the measurement matrix obtained by the

SMDM method, which is built on the basis of the 2-D SCS framework.

- In the framework of 2-D SCS and SMDM, the SCS greedy algorithm of structured sparsity adaptive matching pursuit (S-SAMP) is proposed to recover the NBI in MIMO systems. The proposed S-SAMP algorithm achieves better robustness and efficiency than the classical CS algorithm SAMP and *a priori*-aided SAMP [4], [18], without cooperatively exploiting the 2-D NBI correlations.

The rest of this paper is organized as follows: The system model of the MIMO system as well as the NBI model is described in Section II. Section III presents the main contribution of this paper, including the proposed SMDM method and the S-SAMP algorithm for NBI recovery in MIMO systems. The performance of the proposed method is theoretically analyzed in Section IV. Simulation results are demonstrated in Section V to validate the proposed method, followed by the conclusion.

Notations: Matrices and column vectors are denoted by bold-face letters; $(\cdot)^\dagger$ and $(\cdot)^H$ denote the pseudo-inversion operation and conjugate transpose, respectively; $\|\cdot\|_r$ represents the ℓ_r -norm operation; $\mathbf{v}|_\Omega$ denotes the entries of vector \mathbf{v} in the set of Ω ; $\text{Max}(\mathbf{v}, T)$ denotes the indexes of the T largest entries of vector \mathbf{v} ; \mathbf{A}_Ω and $\mathbf{A}|_\Omega$ represent the submatrices comprised of the Ω columns and Ω rows of matrix \mathbf{A} , respectively; $(\mathbf{A})_{i,j}$ denotes the (i, j) th entry of \mathbf{A} ; Ω^c denotes the complementary set of Ω ; and $\mathbb{E}_X\{\cdot\}$ denotes the mathematical expectation on a random variable X .

Acronyms: The following are the acronyms used in this paper: CS: compressed sensing; SCS: structured compressed sensing; TDM: temporal differential measurement; SMDM: spatial multiple differential measuring; SAMP: sparsity adaptive matching pursuit; S-SAMP: structured SAMP; MIMO: multiple-input multiple-output; MISO: multiple-input single-output; SISO: single-input single-output; NBI: narrowband interference; TS: training sequence; INR: interference-to-noise ratio.

II. SYSTEM MODEL

The NBI signal that interferes with MIMO systems is typically a sparse signal, whose detailed modeling is given as follows. Following the NBI model, the model of typical MIMO systems that suffers from NBI is presented.

A. NBI Signal Model

The frequency-domain NBI signal $\tilde{\mathbf{e}}_i = [\tilde{e}_{i,0}, \tilde{e}_{i,1}, \dots, \tilde{e}_{i,N-1}]^T$, which is interfering with the i th transmitted TS or OFDM symbol with N subcarriers, is a sparse signal usually modeled by a superposition of tone interferers [19]. The sparsity level of the NBI is denoted by K , which is defined as the number of nonzero entries, and is much smaller than the signal dimension, i.e., $K \ll N$. According to the CS theory, the sparsity level should not be too large so that the NBI could be accurately recovered from the undersampled measurement data [15]. The sparsity level also determines the amount of measurement data that is required by the CS method to guarantee the sparse recovery. In practical MIMO systems, since there might not be so many interferers at the same

band of interest [20], the NBI signal can be well assumed to be a strictly sparse signal model. The support of the NBI $\Omega_i = \{k | \tilde{e}_{i,k} \neq 0, k = 0, 1, \dots, N-1\}$ is the set of the locations of nonzero entries. The interference-to-noise ratio (INR) is adopted as an indicator of the NBI intensity compared with the background noise and is defined as $\mathbb{E}_{\tilde{\mathbf{e}}_i} \{\mathcal{P}_e\} / \sigma^2$, with the average power $\mathcal{P}_e = \sum_{k \in \Omega_i} |\tilde{e}_{i,k}|^2 / K$ and the variance of the additive white Gaussian noise (AWGN) σ^2 . After the inverse discrete Fourier transform (IDFT) of $\tilde{\mathbf{e}}_i$, the corresponding time-domain NBI vector \mathbf{e}_i of length M is obtained as $\mathbf{e}_i = \mathbf{F}_M \tilde{\mathbf{e}}_i$, where the partial IDFT matrix $\mathbf{F}_M \in \mathbb{C}^{M \times N}$ is given by

$$\mathbf{F}_M = \frac{1}{\sqrt{N}} [\gamma_0 \quad \gamma_1 \quad \dots \quad \gamma_{N-1}] \quad (1)$$

where γ_k is a vector with the n th element of $\exp(j2\pi kn/N)$, $n = 0, 1, \dots, M-1$, and M is the length of each TS. The locations of the nonzero entries of the NBI signal can be randomly distributed in all the OFDM subcarriers, and the sparsity level is arbitrary. Without loss of generality, the random distribution of the NBI support is applicable for practical wireless channels [21].

In the development of a more effective NBI recovery scheme, the 2-D SCS framework where both the temporal and spatial correlations in a MIMO-OFDM system are exploited is proposed in this paper. The temporal correlation is that the NBI signal remains quasi-static during a certain number of consecutive transmitted symbols. This is based on the fact that NBI in wireless systems is commonly generated by electric-device nonlinearity emission, amateur radio-frequency ingress, or wireless interferers working at relatively fixed frequencies [11], [20]. The spatial correlation of the NBI in MIMO systems is that the NBI supports (the set of nonzero entry locations) at N_r receive antennas are assumed to share the same sparse pattern $\Omega^{(1)} = \Omega^{(2)} = \dots = \Omega^{(N_r)} = \Omega$ [22], since the distance between different receive antennas in the MIMO system is short enough so that the NBI frequencies are spatially correlated.

B. MIMO System Model

In MIMO systems, repeated training sequences are adopted for synchronization and channel estimation, such as in the preamble of the IEEE 802.11 series standards [1], [2]. Without loss of generality, the repeated training sequences specified by the IEEE 802.11p standard [2] are adopted as an instance to demonstrate the mechanism of SMDM, which is shown in Fig. 1. Typically, a 2×2 MIMO system configured in the IEEE 802.11p standard is investigated in this paper, whereas the proposed scheme is also applicable in arbitrary $N_t \times N_r$ MIMO systems. At each transmit antenna, a group of D identical training sequences is sent continuously, with each denoted as $\mathbf{c}^{(t)} = [c_0^{(t)}, c_1^{(t)}, \dots, c_{M-1}^{(t)}]^T$ for the t th transmit antenna and having the identical length M . All the N_t groups of training sequences are sent simultaneously at N_t transmit antennas. After being transmitted over the $N_t \times N_r$ wireless MIMO channel [23] with the channel impulse response $\mathbf{h}^{(tr)} = [h_0^{(tr)}, h_1^{(tr)}, \dots, h_{L-1}^{(tr)}]^T$ between the t th transmit antenna and the r th receive antenna, where $\mathbf{h}^{(tr)}$ is assumed to be invari-

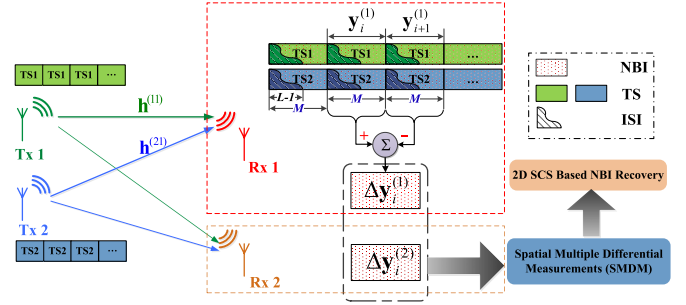


Fig. 1. Two-dimensional SCS-based NBI recovery through SMDM in MIMO systems.

ant during temporally adjacent training sequences [24], the received i th TS impacted by the NBI at the r th receive antenna $\mathbf{y}_i^{(r)} = [y_{i,0}^{(r)}, y_{i,1}^{(r)}, \dots, y_{i,M-1}^{(r)}]^T$, $i = 1, 2, \dots, D$ is given by

$$\mathbf{y}_i^{(r)} = \mathbf{F}_M \tilde{\mathbf{e}}_i^{(r)} + \mathbf{w}_i^{(r)} + \sum_{t=1}^{N_t} \Phi^{(t)} \mathbf{h}^{(tr)} \quad (2)$$

where $\tilde{\mathbf{e}}_i^{(r)}$ denotes the frequency-domain NBI vector for the i th TS at the r th receive antenna, and \mathbf{w}_i is the AWGN vector with zero mean and variance of σ^2 . At the r th receive antenna, the received TS components from the N_t transmit antennas are denoted by $\sum_{t=1}^{N_t} \Phi^{(t)} \mathbf{h}^{(tr)}$ in (2), with the matrix $\Phi^{(t)} \in \mathbb{C}^{M \times L}$ given by

$$\Phi^{(t)} = \begin{bmatrix} c_0^{(t)} & c_{M-1}^{(t)} & c_{M-2}^{(t)} & \dots & c_{M-L+1}^{(t)} \\ c_1^{(t)} & c_0^{(t)} & c_{M-1}^{(t)} & \dots & c_{M-L+2}^{(t)} \\ \vdots & \vdots & \vdots & \ddots & \vdots \\ c_{M-1}^{(t)} & c_{M-2}^{(t)} & c_{M-3}^{(t)} & \dots & c_{M-L}^{(t)} \end{bmatrix}_{M \times L} \quad (3)$$

At each receive antenna, the received signal of the i th TS is given in the form of (2), including the superposition of the received N_t i th training sequences from N_t transmit antennas, the NBI signal, and the background AWGN. The proposed SMDM method will first acquire a one-dimensional (1-D) differential measurement of the NBI exploiting the temporal correlation from each receive antenna and then fully utilizes the spatial correlation of the NBI at the N_r receive antennas and implement the multiple differential measuring of the NBI for the 2-D SCS-based NBI recovery, which is described in detail in the following section.

III. TWO-DIMENSIONAL STRUCTURED COMPRESSED SENSING-BASED NARROWBAND INTERFERENCE RECOVERY IN MULTIPLE-INPUT MULTIPLE-OUTPUT SYSTEMS

How to acquire the measurement matrix of the NBI with 2-D correlations to build up the SCS model is vital. Here, the SMDM method is first proposed to accomplish this task. Afterward, a novel SCS-based greedy algorithm, i.e., S-SAMP, is presented to efficiently recover the SCS optimization problem set up by SMDM.

A. Spatial Multiple Differential Measurements of the NBI

According to the CS theory, obtaining the measurement vector of the NBI signal is crucial for CS algorithms [15]. It has

been proved that using CS algorithms, a sparse vector will be exactly recovered from low-rate sampled measurements in the presence of power-constrained background AWGN [25]. Nevertheless, the TS or data components with much higher power than AWGN should be excluded to ensure effective recovery. This is a difficult task for conventional schemes since the NBI signal is messed up with data or training sequences in both time and frequency domains and difficult to measure separately. To achieve this goal, a novel TDM method has been proposed in our previous work [4] to obtain the measurement vector simply by the differential operation between adjacent received training sequences. For MIMO systems considered in this paper, as shown in Fig. 1, the NBI differential measurement vector $\Delta \mathbf{y}_i^{(r)}$ for the r th receive antenna can be similarly acquired by subtracting $\mathbf{y}_{i+1}^{(r)}$ from $\mathbf{y}_i^{(r)}$ given by (2) to exclude the common received TS components $\sum_{t=1}^{N_t} \Phi^{(t)} \mathbf{h}^{(tr)}$, which yields the following CS measurement equation:

$$\Delta \mathbf{y}_i^{(r)} = \mathbf{F}_M \Delta \tilde{\mathbf{e}}_i^{(r)} + \Delta \mathbf{w}_i^{(r)} \quad (4)$$

where $\Delta \mathbf{y}_i^{(r)} = \mathbf{y}_i^{(r)} - \mathbf{y}_{i+1}^{(r)}$, $\Delta \mathbf{w}_i^{(r)} = \mathbf{w}_i^{(r)} - \mathbf{w}_{i+1}^{(r)}$, and the NBI differential vector at the r th receive antenna $\Delta \tilde{\mathbf{e}}_i^{(r)} \in \mathbb{C}^N$ is denoted as

$$\Delta \tilde{\mathbf{e}}_i^{(r)} = \tilde{\mathbf{e}}_i^{(r)} - \tilde{\mathbf{e}}_{i+1}^{(r)} = \left[\Delta \tilde{e}_{i,0}^{(r)}, \Delta \tilde{e}_{i,1}^{(r)}, \dots, \Delta \tilde{e}_{i,N-1}^{(r)} \right]^T. \quad (5)$$

It is noted that the differential AWGN $\Delta \mathbf{w}_i^{(r)}$ in (4) is the addition of two AWGN variables, which results in an AWGN variable with only a power increase compared with the original background noise. However, it has hardly any impact on the effectiveness of the proposed method. It is proved in [15] and [25] that it is highly probable to recover the sparse signal accurately in the presence of the power constraint of the background noise. Moreover, the power of the practical NBI is much larger than that of AWGN in the frequency domain, which leads to high INR and facilitates the recovery of the NBI. The simulation results are also reported in Section V to show the effectiveness and accuracy of NBI recovery in the presence of the background AWGN.

Due to its temporal correlation, the NBI signal remains invariant during adjacent training sequences, and thus, the time-domain NBI vector at the $(i+1)$ th TS $\mathbf{e}_{i+1}^{(r)}$ is equal to the time-domain NBI vector at the i th TS $\mathbf{e}_i^{(r)}$ delayed by Δl samples, where $\Delta l = M$ is the distance between the two adjacent training sequences. Hence, the frequency-domain NBI vector at the $(i+1)$ th TS $\tilde{\mathbf{e}}_{i+1}^{(r)}$ should be $\tilde{\mathbf{e}}_i^{(r)}$ with a phase shift, i.e.,

$$\tilde{e}_{i+1,k}^{(r)} = \tilde{e}_{i,k}^{(r)} \exp\left(\frac{j2\pi k \Delta l}{N}\right), k = 0, 1, \dots, N-1. \quad (6)$$

Here, (6) is the very temporal correlation of the NBI between adjacent training sequences that facilitates the TDM of the NBI, as well as the proposed SMDM framework. Consequently, the entries of the NBI differential vector in (5) are given by

$$\Delta \tilde{e}_{i,k}^{(r)} = \tilde{e}_{i,k}^{(r)} \left(1 - \exp\left(\frac{j2\pi k \Delta l}{N}\right)\right), k = 0, 1, \dots, N-1. \quad (7)$$

The unknown sparse NBI differential vector is estimated from only a 1-D measurement vector by solving (4) using CS algorithms in our previously proposed method [4]. However, this approach might suffer from large NBI sparsity levels, strong background noise, and short length of the measurement vector in severe circumstances.

In the proposed framework of 2-D SCS and SMDM, the spatial correlation as well as the temporal correlation of the NBI signal is taken full advantage of to improve the stability of NBI recovery for MIMO systems. Recall that one measurement vector at the i th received TS given by (4) is acquired for each receive antenna using the previously proposed TDM method. Now, in the proposed SMDM method, considering the N_r measurement vectors at the i th received TS from the N_r receive antennas, with each having the form of the CS sparse measurement model given by (4), we obtain the following SCS measurement equation:

$$\Delta \mathbf{Y} = \left[\Delta \mathbf{y}_i^{(1)}, \Delta \mathbf{y}_i^{(2)}, \dots, \Delta \mathbf{y}_i^{(N_r)} \right]_{M \times N_r} = \mathbf{F}_M \Delta \tilde{\mathbf{E}} + \Delta \mathbf{W} \quad (8)$$

where $\Delta \tilde{\mathbf{E}} = [\Delta \tilde{\mathbf{e}}_i^{(1)}, \Delta \tilde{\mathbf{e}}_i^{(2)}, \dots, \Delta \tilde{\mathbf{e}}_i^{(N_r)}]$ are the spatially jointly sparse matrix of the NBI whose columns share the same support Ω (i.e., NBI supports at the N_r receive antennas are the same), whereas the values of the nonzero entries in the same row of the matrix might be different from each other. $\Delta \mathbf{W} = [\Delta \mathbf{w}_i^{(1)}, \Delta \mathbf{w}_i^{(2)}, \dots, \Delta \mathbf{w}_i^{(N_r)}]$ is the AWGN matrix. Consequently, the formulated mathematical model (8) precisely complies with the newly developed theory of SCS [17].

According to the SCS theory, it is proved that the jointly sparse vectors within $\Delta \tilde{\mathbf{E}}$ (the columns of $\Delta \tilde{\mathbf{E}}$) will be simultaneously recovered accurately by solving the convex optimization problem, which is deduced from the SCS measurement equation (8), as follows [17]:

$$\Delta \hat{\tilde{\mathbf{E}}} = \arg \min_{\Delta \tilde{\mathbf{E}} \in \mathbb{C}^{N \times N_r}} \|\Delta \tilde{\mathbf{E}}\|_{p,q}, \text{ s.t. } \|\Delta \mathbf{Y} - \mathbf{F}_M \Delta \tilde{\mathbf{E}}\|_{p,q} \leq \epsilon^2 \quad (9)$$

where ϵ^2 denotes the power constraint of the background AWGN $\Delta \mathbf{W}$, and the $\ell_{p,q}$ norm of the matrix $\Delta \tilde{\mathbf{E}}$ is defined by

$$\|\Delta \tilde{\mathbf{E}}\|_{p,q} = \left(\sum_m \|\Delta \tilde{\mathbf{E}}_m\|_p^q \right)^{\frac{1}{q}} \quad (10)$$

with $\Delta \tilde{\mathbf{E}}_m$ being the m th row of $\Delta \tilde{\mathbf{E}}$. The $\ell_{2,0}$ norm is adopted [17], with $\epsilon^2 = N_r \sigma^2$ accordingly. Note that the previously proposed TDM approach without exploiting the spatial correlation can be regarded as a special case of the newly proposed SCS-based SMDM framework with $N_r = 1$ in (8) and (9).

Greedy CS algorithms could be implemented to solve the 1-D convex optimization problem (4) induced by the TDM method, such as the classical SAMP [18] dealing with sparse recovery with unknown sparsity levels. Using the TDM method with the SAMP algorithm, the NBI $\Delta \tilde{\mathbf{e}}_i^{(r)}$ is recovered and canceled at each receive antenna separately without cooperative reconstruction of NBI from multiple receive antennas that exploits the spatial correlation in MIMO systems. However, since SAMP

is aimed at the classical CS-based recovery using only 1-D measurement, it might become vulnerable in severe conditions. To solve this problem, the spatial correlation of the NBI is fully exploited to improve the stability and accuracy of SAMP for the MIMO system. Under the 2-D SCS-based SMDM framework, we propose the S-SAMP algorithm to effectively solve the multidimensional convex optimization problem in (9) and reconstruct the spatially jointly sparse matrix $\Delta\hat{\mathbf{E}}$ accurately, which is introduced in detail in the following section.

B. SCS-Based Greedy Algorithm of Structured SAMP

The pseudocode of the proposed S-SAMP is summarized in **Algorithm 1**. The inputs of **Algorithm 1** are the measurement matrix $\Delta\mathbf{Y}$, the observation matrix $\Psi = \mathbf{F}_M$, and the iteration step size δ of the test sparsity level K_t . The iterations are composed of multiple stages, and K_t is increased by δ when the stage switches. The output of *Algorithm 1* is the final output support $\hat{\Omega}$ and the recovered jointly sparse matrix $\Delta\hat{\mathbf{E}}$ of the NBI s.t. $\Delta\hat{\mathbf{E}}|_{\hat{\Omega}} = \Psi_{\hat{\Omega}}^\dagger \Delta\mathbf{Y}$, $\Delta\hat{\mathbf{E}}|_{\hat{\Omega}^c} = \mathbf{0}$.

Algorithm 1 S-SAMP for NBI Recovery in the MIMO System

Input:

- 1) Measurement matrix $\Delta\mathbf{Y}$
- 2) Observation matrix $\Psi = \mathbf{F}_M$
- 3) Step size δ .

Initialization:

- 1: $\Delta\hat{\mathbf{E}}^{(0)} \leftarrow \mathbf{0}_{N \times N_r}$; $\mathbf{R}^{(0)} \leftarrow \Delta\mathbf{Y}$
- 2: $\Omega^{(0)} \leftarrow \emptyset$; $K_t \leftarrow \delta$
- 3: $k \leftarrow 1$; $j \leftarrow 1$

Iterations:

- 4: **repeat**
- 5: $\mathbf{v} \in \mathbb{C}^N$ s.t. $v_i = \sum_{j=1}^{N_r} |(\Psi^H \mathbf{R}^{(k-1)})_{i,j}|$
- 6: $S_k \leftarrow \text{Max}\{\mathbf{v}, K_t\}$ {Preliminary test}
- 7: $C_k \leftarrow \Omega^{(k-1)} \cup S_k$ {Make candidate list}
- 8: $\mathbf{u} \in \mathbb{C}^{|C_k|}$ s.t. $u_i = \sum_{j=1}^{N_r} |(\Psi_{C_k}^\dagger \Delta\mathbf{Y})_{i,j}|$
- 9: $\Omega_t \leftarrow \text{Max}\{\mathbf{u}, K_t\}$ {Temporary final list}
- 10: $\Delta\hat{\mathbf{E}}^{(k)}|_{\Omega_t} \leftarrow \Psi_{\Omega_t}^\dagger \Delta\mathbf{Y}$; $\Delta\hat{\mathbf{E}}^{(k)}|_{\Omega_t^c} \leftarrow \mathbf{0}$
- 11: $\mathbf{R}_t \leftarrow \Delta\mathbf{Y} - \Psi_{\Omega_t} \Psi_{\Omega_t}^\dagger \Delta\mathbf{Y}$ {Compute residue}
- 12: **if** $\|\mathbf{R}_t\|_{2,0} \geq \|\mathbf{R}^{(k-1)}\|_{2,0}$ **then**
- 13: $T \leftarrow T + \delta$ {Stage switching}
- 14: **else**
- 15: $\Omega^{(k)} \leftarrow \Omega_t$; $\hat{\Omega} \leftarrow \Omega_t$; $\mathbf{R}^{(k)} \leftarrow \mathbf{R}_t$
- 16: $k \leftarrow k + 1$ {Same stage, next iteration}
- 17: **end if**
- 18: **until** $\|\mathbf{R}_t\|_{2,0} < \epsilon^2$

Output:

- 1) Final output support $\hat{\Omega}$
 - 2) Recovered spatially jointly sparse matrix $\Delta\hat{\mathbf{E}}$, s.t. $\Delta\hat{\mathbf{E}}|_{\hat{\Omega}} = \Psi_{\hat{\Omega}}^\dagger \Delta\mathbf{Y}$, $\Delta\hat{\mathbf{E}}|_{\hat{\Omega}^c} = \mathbf{0}$
-

It is observed from *Algorithm 1* that the spatial correlation of the NBI is fully exploited in S-SAMP by summing up the values of the N_r columns of the measurement matrix $\Delta\mathbf{Y}$ to pick out the maximum K_t entries as the candidate support list

in each iteration instead of picking from only one measurement vector in classical SAMP [18]. Under the 2-D SCS-based SMDM framework, S-SAMP takes full advantage of the spatial multiple differential measurements to enhance the robustness of NBI recovery. Particularly under severe conditions with short measurement vector, large background noise intensity, or higher sparsity levels, S-SAMP ensures better performance than classical CS algorithms, which is demonstrated by simulations in Section IV.

C. Subsequent NBI Cancellation for MIMO Systems

The r th column of the recovered jointly sparse matrix $\Delta\hat{\mathbf{E}}$ of the NBI is the recovered NBI differential vector $\Delta\hat{\mathbf{e}}_i^{(r)}$ related to the r th receive antenna. Hence, according to (5) and (7), the original frequency-domain NBI vector $\tilde{\mathbf{e}}_i^{(r)}$ associated to the i th received TS $\mathbf{y}_i^{(r)}$ at the r th receive antenna can be acquired from $\Delta\hat{\mathbf{e}}_i^{(r)}$ by

$$\tilde{\mathbf{e}}_{i,k}^{(r)} = \frac{\Delta\hat{\mathbf{e}}_{i,k}^{(r)}}{\left(1 - \exp\left(\frac{j2\pi k \Delta l}{N}\right)\right)}, k = 0, 1, \dots, N-1. \quad (11)$$

Finally, the frequency-domain NBI vector $\tilde{\mathbf{e}}_n'^{(r)} = [\tilde{e}'_{n,0}, \tilde{e}'_{n,1}, \dots, \tilde{e}'_{n,N-1}]^T$ associated to the received n th OFDM symbol in the payload at the r th receive antenna is similarly acquired by

$$\tilde{\mathbf{e}}_{n,k}'^{(r)} = \tilde{\mathbf{e}}_{i,k}^{(r)} \cdot \exp\left(\frac{j2\pi k \Delta d_{i,n}}{N}\right), k = 0, 1, \dots, N-1 \quad (12)$$

where $\{\Delta d_{i,n} = (n-1)F + (D-i+1)M\}_{i=2}^{D-1}$ is the distance between the i th received TS $\mathbf{y}_i^{(r)}$ and the n th OFDM symbol with the frame length of F . Afterward, the recovered NBI signal is canceled from the received OFDM symbol for each of the N_r receive antennas.

IV. PERFORMANCE EVALUATION

This section gives an evaluation on the performance of the proposed method, including the analysis of the computational complexity of the algorithm, and a brief introductory analysis of the restricted isometry property of the adopted observation matrix.

A. Computational Complexity Analysis

The computational complexity of the proposed 2-D SCS-based SMDM method using the proposed S-SAMP algorithm mainly includes the following two parts.

- 1) SMDM: The complexity of each 1-D CS measurement vector acquisition at each receive antenna is $\mathcal{O}(M)$; hence, the complexity of the SMDM operation for obtaining multiple measurement vectors at the N_r receive antennas is $\mathcal{O}(N_r M)$.
- 2) S-SAMP: The SCS greedy algorithm contributes the major complexity. For each iteration, the complexity consists of two parts: the inner product between the observation

matrix Ψ and the residue matrix $\mathbf{R}^{(k-1)}$ has complexity of $\mathcal{O}(N_r MN)$; the equivalent LS problem $\Delta \hat{\mathbf{E}}^{(k)}|_{\Omega_t} \leftarrow \Psi_{\Omega_t}^\dagger \Delta \mathbf{Y}$ requires the complexity $\mathcal{O}(N_r MK)$, which is distinguished from that of the classical SAMP algorithm in that each iteration has been extended to N_r multiple dimensions. The upper bound of the total number of iterations is K in S-SAMP; hence, the total complexity of S-SAMP is on the order of $\mathcal{O}(KN_r M(N + K))$.

To sum up, the total complexity of the proposed NBI cancellation approach is on the order of $\mathcal{O}(N_r M + KN_r M(N + K))$.

B. Brief Introductory Analysis on Restricted Isometry Property

The observation matrix should satisfy the restricted isometry property to solve the CS problem accurately according to the probabilistic theory of sparse signal recovery [26]. An $M \times N$ matrix \mathbf{A} is considered to obey the restricted isometry property with parameters K and δ_K if

$$(1 - \delta_K) \|\mathbf{x}\|_2^2 \leq \|\mathbf{A}\mathbf{x}\|_2^2 \leq (1 + \delta_K) \|\mathbf{x}\|_2^2 \quad (13)$$

for any K -sparse vector \mathbf{x} (K -sparse means its sparsity level is K), where the parameter $0 \leq \delta_K < 1$ is the restricted isometry constant. With the decrease of δ_K , the isometric property of matrix \mathbf{A} becomes more restricted and closer to the strict orthogonal isometric property for matrix \mathbf{A} when $\delta_K = 0$. Hence, the restricted isometry property can also be regarded as the indicator of the orthogonality extent of the matrix. Considering the observation matrix \mathbf{F}_M used in the proposed SMDM method, the semiorthogonal property is inherent due to its specific structure. It is not difficult to prove that the cross-correlation values of the columns of \mathbf{F}_M are relatively small compared with the autocorrelation value of 1. We can regard this property as the *semiorthogonal property*, which indicates that the observation matrix \mathbf{F}_M of the proposed method satisfies the restricted isometry property requirements properly with a fairly small restricted isometry property constant δ_K .

V. SIMULATION RESULTS AND DISCUSSIONS

The performance of the proposed 2-D SCS-based SMDM method with the proposed S-SAMP algorithm for NBI recovery in wireless MIMO systems is evaluated through simulations. The NBI recovery performance of the previously proposed classical CS-based TDM method with the SAMP algorithm, which is implemented at each receive antenna separately, is also evaluated using the same MIMO system setup for comparison (as described in Section III-A, it is equivalent to the NBI recovery process in the MISO or the SISO system). Typically, the simulation setup is configured according to the wireless access in vehicular environment MIMO systems specified by the IEEE 802.11p standard [2]. The OFDM subcarrier number $N = 64$, and the length of each TS $M = 16$. The number of repeated training sequences sent by each transmit antenna is $D = 5$. The 2×2 MIMO or 4×4 MIMO multipath channel [23] in the presence of NBI is adopted. The low-density parity-check code with a code length of 1944 bits and a code rate of 1/2, as well as the 64-quadrature amplitude modulation as specified in [1] are adopted.

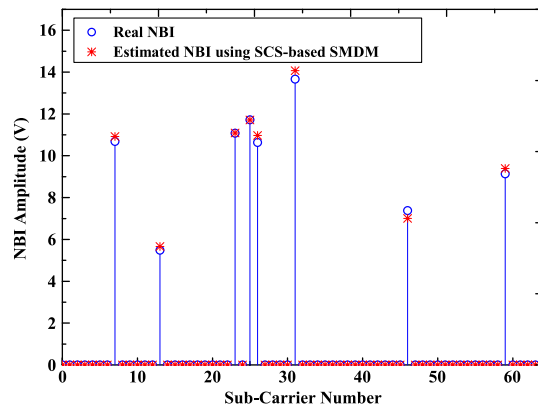


Fig. 2. Performance of one realization of NBI recovery using the 2-D SCS-based SMDM scheme with S-SAMP.

The performance of one realization of the NBI recovery using the proposed 2-D SCS-based SMDM scheme with the S-SAMP algorithm for the 2×2 MIMO wireless access in the vehicular environment system is shown in Fig. 2, when the sparsity level $K = 4$ and INR = 30 dB. Without loss of generality, we demonstrate the actual and estimated NBI signals at one of the receive antennas. The NBI at one certain receive antenna is recovered from the measurement matrix constituted by the differential measurements at $N_r = 2$ receive antennas. The result in Fig. 2 implies that the NBI estimation precisely matches the actual NBI signal.

The mean square error (MSE) of NBI recovery is shown in Fig. 3. In the 2×2 MIMO wireless access in the vehicular environment system, the SMDM scheme with the S-SAMP algorithm, and the previously proposed TDM scheme with the SAMP algorithm are compared, with the sparsity level $K = 4$ and $K = 8$. The theoretical Cramer–Rao lower bound (CRLB) of $2\sigma^2(NK/M)$ [4] is depicted as the benchmark. The proposed SMDM scheme with S-SAMP achieves the MSE of 10^{-3} with the INR of 17.5 and 24.6 dB at the sparsity level $K = 4$ and $K = 8$, respectively, which has a 2.5-dB gain over the TDM method with SAMP. With the increase of INR, the MSE of SMDM asymptotically approaches the CRLB, verifying the recovery accuracy. Moreover, the introduction of SMDM will reduce the requirement of the length of the measurement vector from $\mathcal{O}(K \log_2(N/K))$ in the classical CS to $\mathcal{O}(K)$ in SCS [22].

The NBI recovery probability versus the sparsity level K is shown in Fig. 4. The recovery probability is defined as the frequency of successful NBI recovery, i.e., the frequency of $\text{MSE} < 10^{-2}$. It is noted that the SMDM scheme with S-SAMP for 2×2 MIMO and 4×4 MIMO reaches a recovery probability of 0.9 at $K > 7$ and $K > 10$, respectively, which indicates that the proposed SMDM method exploiting the spatial correlation can recover the NBI signal at larger sparsity levels and is more robust against the variance of the sparsity level than the previously proposed TDM method with the SAMP algorithm in the MIMO system.

To demonstrate the effects of different measurement vector lengths on the NBI recovery performance, we assume that the length of each TS M used as the measurement vector is variant

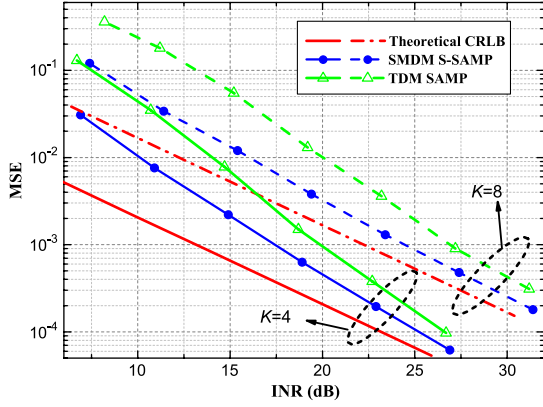


Fig. 3. MSE of NBI recovery versus INR for the 2-D SCS-based SMDM scheme with S-SAMP and the 1-D CS-based TDM scheme with SAMP for the 2×2 MIMO system.

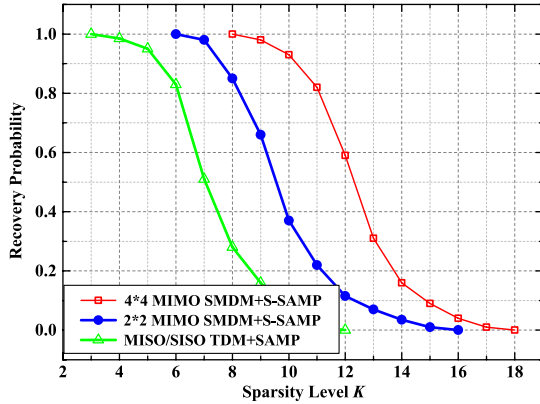


Fig. 4. NBI recovery probability versus sparsity level K for the 2-D SCS-based SMDM S-SAMP and 1-D CS-based TDM SAMP schemes.

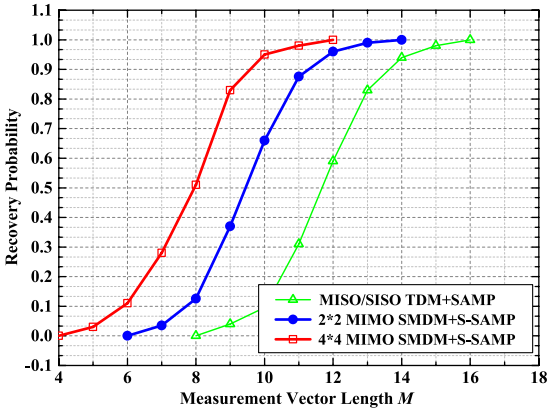


Fig. 5. NBI recovery probability versus measurement vector length M for the 2-D SCS-based SMDM S-SAMP and 1-D CS-based TDM SAMP schemes.

in this case and simulate the corresponding performance. This way, the recovery probability of both the SMDM method with S-SAMP and the TDM method with SAMP versus the measurement vector length M is shown in Fig. 5. It can be noted from Fig. 5 that to reach the successful NBI recovery probability of 0.90, the 4×4 MIMO and 2×2 MIMO SMDM method with S-SAMP only require $M = 9$ and $M = 11$ measurement vector length (measurement samples), whereas longer measurement

TABLE I
AVERAGE NUMBER OF ITERATIONS TO REACH SUCCESSFUL NBI RECONSTRUCTION ($MSE < 10^{-3}$)

Sparsity Level	S-SAMP	SAMP
4	2.42	3.36
8	3.79	7.14
12	8.63	12.48

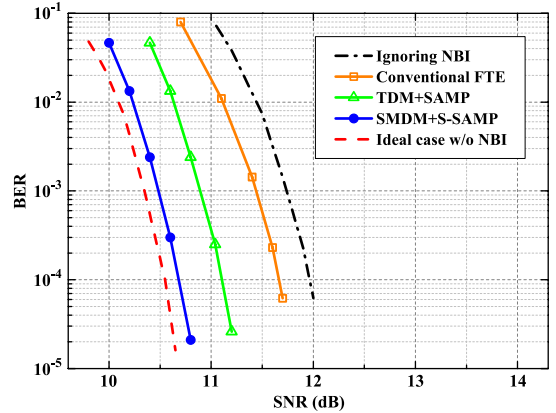


Fig. 6. BER performance comparison of different NBI mitigation schemes for the 2×2 MIMO wireless access in the vehicular environment system.

vector $M = 14$ is required by the MISO/SISO TDM method with SAMP. It can be inferred that the proposed SMDM method takes full advantage of the spatial correlation in MIMO systems based on the SCS theory, making the NBI easier to recover and cancel with less measurement data. Hence, using the proposed SMDM method, shorter overhead TS in the IEEE 802.11p standard specified preamble is needed for NBI cancellation.

To quantitatively measure the execution time of the proposed SCS greedy algorithm S-SAMP and the classical CS greedy algorithm SAMP, the average number of iterations using S-SAMP and SAMP for NBI recovery is summarized in Table I, where the average value is calculated from 10^6 times of NBI reconstruction simulations. It can be noted that the average iteration number to reach the same criterion ($MSE < 10^{-3}$, $INR = 30$ dB) for S-SAMP is significantly smaller than that of SAMP in case of different sparsity levels. One can infer from Table I that the convergence rate of NBI recovery will be much higher using the proposed SMDM method and the S-SAMP algorithm that exploits the MIMO spatial correlation based on the SCS theory.

The bit error rate (BER) performances of different NBI mitigation schemes over the 2×2 MIMO channel in the presence of NBI are shown in Fig. 6, including the proposed SMDM scheme with S-SAMP, as well as the conventional frequency threshold excision method and the TDM method with SAMP for comparison. The case ignoring NBI and the ideal case without NBI are depicted as benchmarks. It is observed that the proposed SMDM method with S-SAMP outperforms the conventional frequency threshold excision method and the case ignoring NBI by approximately 0.9 and 1.2 dB, respectively, at the target BER of 10^{-4} in the presence of the NBI with $K = 8$ and $INR = 30$ dB. With the aid of the spatial correlation

under the SCS framework, the SMDM method further achieves a 0.4-dB gain over the previously proposed TDM method. Moreover, the proposed SMDM method is only about 0.1 dB from the ideal curve without NBI, which demonstrates the accuracy and effectiveness of NBI recovery for MIMO systems.

VI. CONCLUSION

In this paper, a novel 2-D SCS-based method of NBI cancellation has been proposed in MIMO systems and validated by both theoretical analysis and computer simulations. Exploiting the spatial and temporal correlations of the NBI, the classical CS algorithm SAMP is improved by the proposed S-SAMP algorithm. The proposed SMDM method is capable of recovering the NBI only using the training sequences in the existing IEEE 802.11 series standards. The proposed 2-D SCS-based SMDM method outperforms conventional NBI mitigation schemes, as well as the classical CS-based TDM method that ignores the spatial correlation, particularly in severe conditions where strong background noise and large NBI sparsity levels are present. The 2-D SCS-based SMDM method requires an even shorter TS length in the IEEE 802.11 preamble for measurements than does the classical CS-based TDM method. Furthermore, apart from the IEEE 802.11 series MIMO systems, the proposed method is also workable in other communication systems adopting repeated training sequences impacted by NBI and in massive MIMO systems.

REFERENCES

- [1] *Wireless LAN Medium Access Control (MAC) and Physical Layer (PHY) Specifications*, IEEE Std. 802.11n, Oct. 2009.
- [2] *IEEE Standard for Information technology—Local and metropolitan area networks—Specific requirements—Part 11: Wireless LAN Medium Access Control (MAC) and Physical Layer (PHY) Specifications Amendment 6: Wireless Access in Vehicular Environments*, IEEE Std. 802.11p, Jul. 2010.
- [3] J. Park, D. Kim, C. Kang, and D. Hong, "Effect of Bluetooth interference on OFDM-based WLAN," in *Proc. IEEE Veh. Technol. Conf.*, Oct. 2003, vol. 2, pp. 786–789.
- [4] S. Liu, F. Yang, W. Ding, and J. Song, "Double kill: Compressive sensing based narrowband interference and impulsive noise mitigation for vehicular communications," *IEEE Trans. Veh. Technol.*, vol. 65, no. 7, pp. 5099–5109, Jul. 2016.
- [5] Y. Matsumoto, M. Takeuchi, K. Fujii, A. Sugiura, and Y. Yamanaka, "Performance analysis of interference problems involving DSSS WLAN systems and microwave ovens," *IEEE Trans. Electromagn. Compat.*, vol. 47, no. 1, pp. 45–53, Feb. 2005.
- [6] Y. Matsumoto, T. Shimizu, T. Murakami, K. Fujii, and A. Sugiura, "Impact of frequency-modulated harmonic noises from PCs on OFDM-based WLAN systems," *IEEE Trans. Electromagn. Compat.*, vol. 49, no. 2, pp. 455–462, May 2007.
- [7] J. Zhang and J. Meng, "Noise resistant OFDM for power-line communication systems," *IEEE Trans. Power Del.*, vol. 25, no. 2, pp. 693–701, Apr. 2010.
- [8] P. Odling, P. Borjesson, T. Magesacher, and T. Nordstrom, "An approach to analog mitigation of RFI," *IEEE J. Sel. Areas Commun.*, vol. 20, no. 5, pp. 974–986, Jun. 2002.
- [9] S. Liu, F. Yang, J. Song, F. Ren, and J. Li, "OFDM preamble design for synchronization under narrowband interference," in *Proc. IEEE ISPLC*, Mar. 2013, pp. 252–257.
- [10] M. Marey and H. Steendam, "Analysis of the narrowband interference effect on OFDM timing synchronization," *IEEE Trans. Signal Process.*, vol. 55, no. 9, pp. 4558–4566, Sep. 2007.
- [11] D. Chi and P. Das, "Effects of nonlinear amplifiers and narrowband interference in MIMO-OFDM with application to 802.11n WLAN," in *Proc. IEEE 2nd ICSPCS*, Dec. 2008, pp. 1–7.
- [12] S. Liu, F. Yang, and J. Song, "An optimal interleaving scheme with maximum time–frequency diversity for PLC systems," *IEEE Trans. Power Del.*, vol. 31, no. 3, pp. 1007–1014, Jun. 2016.
- [13] S. Kai *et al.*, "Impacts of narrowband interference on OFDM-UWB receivers: Analysis and mitigation," *IEEE Trans. Signal Process.*, vol. 55, no. 3, pp. 1118–1128, Mar. 2007.
- [14] R. Nilsson, F. Sjöberg, and J. LeBlanc, "A rank-reduced LMMSE canceller for narrowband interference suppression in OFDM-based systems," *IEEE Trans. Commun.*, vol. 51, no. 12, pp. 2126–2140, Dec. 2003.
- [15] D. Donoho, "Compressed sensing," *IEEE Trans. Inf. Theory*, vol. 52, no. 4, pp. 1289–1306, Apr. 2006.
- [16] A. Gomaa and N. Al-Dhahir, "A sparsity-aware approach for NBI estimation in MIMO-OFDM," *IEEE Trans. Wireless Commun.*, vol. 10, no. 6, pp. 1854–1862, Jun. 2011.
- [17] M. Duarte and Y. Eldar, "Structured compressed sensing: From theory to applications," *IEEE Trans. Signal Process.*, vol. 59, no. 9, pp. 4053–4085, Sep. 2011.
- [18] T. Do, G. Lu, N. Nguyen, and T. Tran, "Sparsity adaptive matching pursuit algorithm for practical compressed sensing," in *Proc. IEEE Asilomar Conf. Signals, Syst., Comput.*, Oct. 2008, pp. 581–587.
- [19] A. Tonello and F. Pecile, "Efficient architectures for multiuser FMT systems and application to power line communications," *IEEE Trans. Commun.*, vol. 57, no. 5, pp. 1275–1279, May 2009.
- [20] A. Oka and L. Lampe, "Compressed sensing reception of bursty UWB impulse radio is robust to narrow-band interference," in *Proc. IEEE Globecom*, Nov./Dec. 2009, pp. 1–7.
- [21] A. Coulson, "Narrowband interference in pilot symbol assisted OFDM systems," *IEEE Trans. Wireless Commun.*, vol. 3, no. 6, pp. 2277–2287, Nov. 2004.
- [22] E. van den Berg and M. Friedlander, "Theoretical and empirical results for recovery from multiple measurements," *IEEE Trans. Inf. Theory*, vol. 56, no. 5, pp. 2516–2527, May 2010.
- [23] R. Stridh, K. Yu, B. Ottersten, and P. Karlsson, "MIMO channel capacity and modeling issues on a measured indoor radio channel at 5.8 GHz," *IEEE Trans. Wireless Commun.*, vol. 4, no. 3, pp. 895–903, May 2005.
- [24] *Guideline for Evaluation of Radio Transmission Technology for IMT-2000*, Rec. Std. ITU-R M. 1225, 1997.
- [25] D. Donoho, M. Elad, and V. Temlyakov, "Stable recovery of sparse overcomplete representations in the presence of noise," *IEEE Trans. Inf. Theory*, vol. 52, no. 1, pp. 6–18, Jan. 2006.
- [26] J. Candès and Y. Plan, "A probabilistic and RIPless theory of compressed sensing," *IEEE Trans. Inf. Theory*, vol. 57, no. 11, pp. 7235–7254, Nov. 2011.



Sicong Liu (S'15) received the B.S.E. degree in electronic engineering from the Department of Electronic Engineering, Tsinghua University, Beijing, China, where he is currently working toward the Ph.D. degree in electronic engineering with the DTV Technology R&D Center.

His research interests include power line communications, broadband transmission techniques, and interference mitigation.



Fang Yang (M'11–SM'13) received the B.S.E. and Ph.D. degrees in electronic engineering from Tsinghua University, Beijing China, in 2005 and 2009, respectively.

He is currently an Associate Professor with the DTV Technology R&D Center, Tsinghua University. His research interests lie in the fields of power line communications, visible light communications, and digital television terrestrial broadcasting.



Wenbo Ding (S'15) received the B.S.E. degree (with distinction) from the Department of Electronic Engineering, Tsinghua University, Beijing, China, in 2011, where he is currently working toward the Ph.D. degree with the DTV Technology R&D Center.

He has published over 20 journal and conference papers. His research interests lie in the field of sparse signal processing and its applications in power line communications, visible light communications, smart grids, and future fifth-generation wireless communications.

Dr. Ding has received the IEEE Scott Helt Memorial Award for the Best Paper published in the IEEE TRANSACTIONS ON BROADCASTING in 2015.



Xianbin Wang (S'98–M'99–SM'06) received the Ph.D. degree in electrical and computer engineering from the National University of Singapore, Singapore, in 2001.

He is a Professor and the Canada Research Chair with the University of Western Ontario, London, ON, Canada. Between July 2002 and December 2007, he was with Communications Research Center Canada (CRC). From January 2001 to July 2002, he was a System Designer with STMicroelectronics.

His current research interests include fifth-generation

networks, adaptive wireless systems, communications security, and locationing technologies.

Dr. Wang is an IEEE Distinguished Lecturer. He has received many awards and recognitions, including Canada Research Chair, CRC President's Excellence Award, the Canadian Federal Government Public Service Award, the Ontario Early Researcher Award, and three IEEE Best Paper Awards. He currently serves as an Editor/Associate Editor for the IEEE WIRELESS COMMUNICATIONS LETTERS, the IEEE TRANSACTIONS ON VEHICULAR TECHNOLOGY, and the IEEE TRANSACTIONS ON BROADCASTING. He also served as an Editor for the IEEE TRANSACTIONS ON WIRELESS COMMUNICATIONS between 2007 and 2011. He has been involved in a number of IEEE conferences, including the Global Communications Conference, the International Conference on Communications, the Wireless Communications and Networking Conference, the Vehicular Technology Conference, the International Conference on Multimedia and Expo, and the Canadian Workshop on Information Theory, in different roles such as Symposium Chair, Tutorial Instructor, Track Chair, Session Chair, and Technical Program Committee Chair.



Jian Song (M'06–SM'10–F'16) received the B.Eng. and Ph.D. degrees in electrical engineering from Tsinghua University, Beijing, China, in 1990 and 1995, respectively.

He worked for the same university upon his graduation and has worked with The Chinese University of Hong Kong, Hong Kong, and the University of Waterloo, Waterloo, ON, Canada, in 1996 and 1997, respectively. He was with Hughes Network Systems, Germantown, MD, USA, for seven years before joining the faculty team at Tsinghua University

in 2005 as a Professor. He is currently the Director of the DTV Technology R&D Center, Tsinghua University. He has published more than 110 peer-reviewed journal and conference papers. He is the holder of two U.S. and more than 20 Chinese patents. He has been working in many different areas of fiber-optic, satellite, and wireless communications, as well as power line communications. His current research interest is in the area of digital TV broadcasting.

Dr. Song is a Fellow of the Institution of Engineering and Technology.